Quantum chemical exploration of PEM fuel cell processes

Bent SØRENSEN
Roskilde University, Energy & Environment Group, Bld. 27.2
Universitetsvej 1, PO Box 260
DK-4000 Roskilde
DENMARK
email: boson@ruc.dk

Abstract
Modelling of fuel cells include several levels of theory: Overall electrical behaviour of the cell may be described by circuit analogue networks, flow of oxygen and hydrogen through the external pipes by fluid dynamics models, while the penetration of these gases through the gas diffusion layer and possibly also the passage of hydrogen ions through the membrane can be described using diffusion models. Finally, the central processes of water splitting near the catalyst layers, by addition of electric energy from the external circuit, or by recombination of oxygen and hydrogen molecules to create electric energy for external use, invite the use of quantum chemical calculations. This communication gives some elements of this ongoing work.

1. Introductory remarks on organic and inorganic water splitting paths

Use of proton exchange membrane (PEM) fuel cells for water splitting by electrolysis is shown schematically in Figure 1. The electricity production from hydrogen and oxygen is basically the same apparatus, with flows reversed and electricity output instead of input. The part of the device amenable to quantum chemical modelling is indicated by a white rectangle and enlarged in Figure 2.

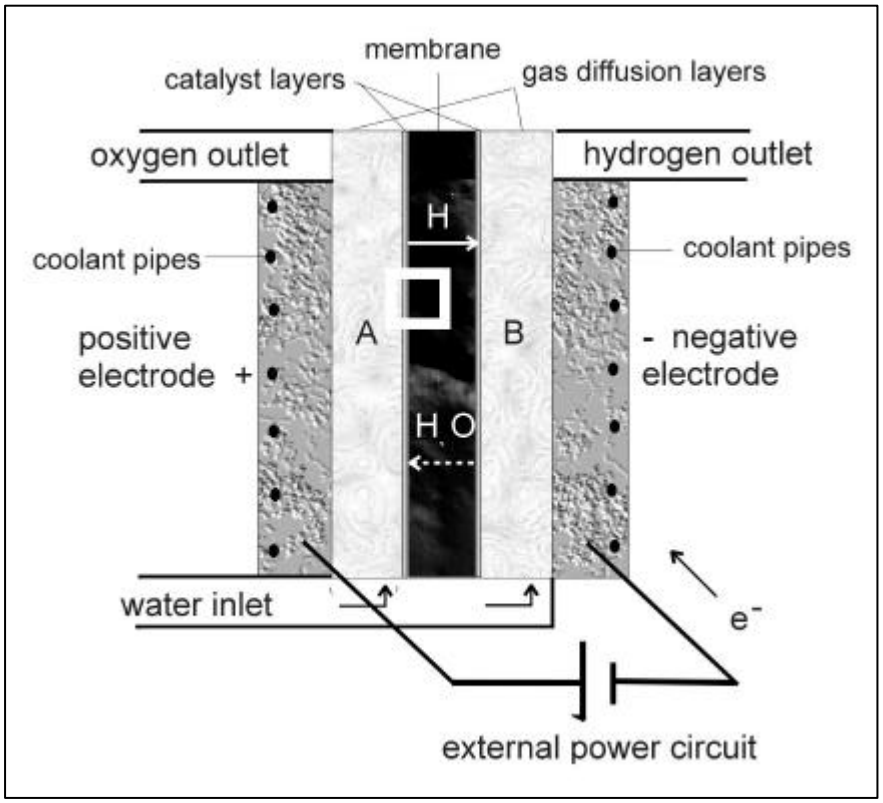

Figure 1. PEM fuel cell with indication of flow direction for use as electrolyser [1]. The white rectangle indicates the area of interest in this work, depicted in more detail in Figure 2.

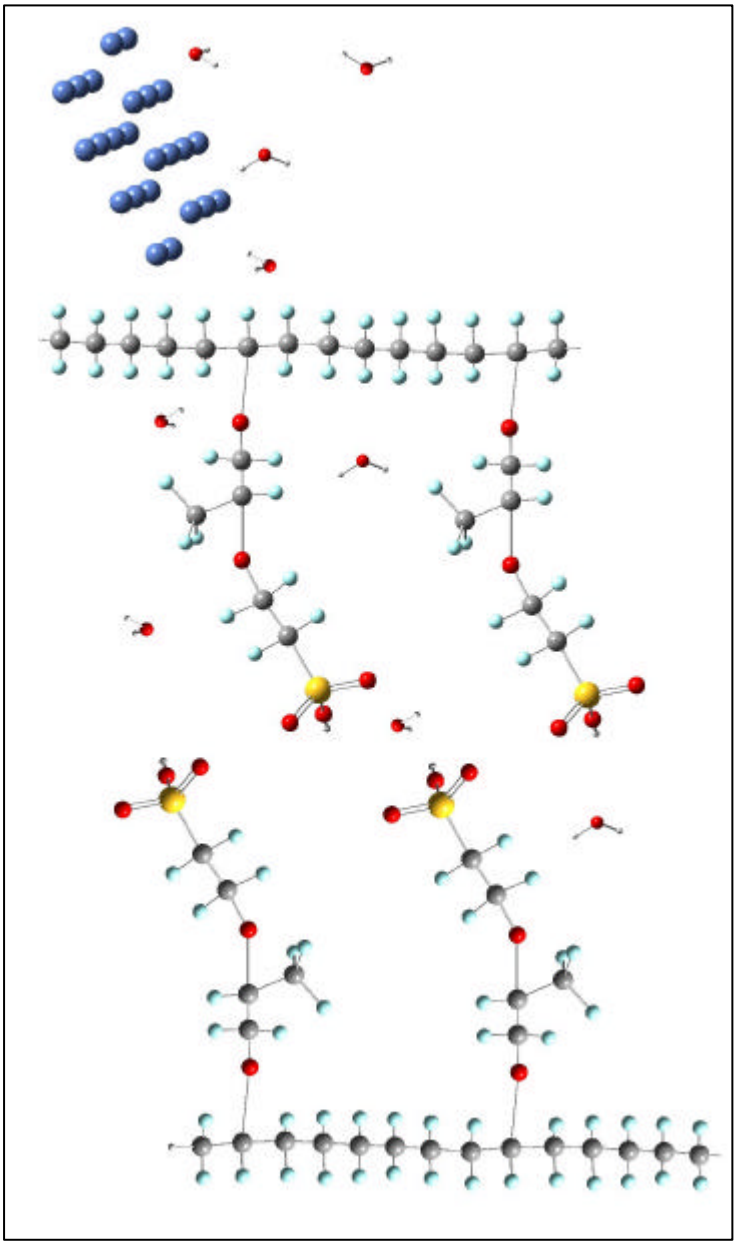

Figure 2. Highly schematic picture of the molecular structure of PEM fuel cell area near the membrane assumed to be of the Nafion [5] type, indicating a: the perfluorinated ionomer membrane indicated as two CF_2 backbones with sidechains ending in HSO_3, b: a nanoparticle (at top of picture) made of a catalyst such as Pt or Ni, and c: spread throughout both the inner and outer membrane area a number of water molecules. Only one "sheet" of the membrane is shown. It is supposed to repeat itself in and out of the paper plane, in the way discussed in the text [1].

It is interesting to compare this type of water splitting device with the photosystem II of plants and many bacteria, in order to reveal similarities and differences in the way water is converted into molecular oxygen and hydrogen ions capable of moving through the system. Figure 3 shows the two photosystems of a cyanobacterium and the intermediate cytochrome cluster, capable of capturing solar energy by a large number of chlorophyll molecules in the two photosystem. The energy derived from solar radiation is in photosystem II used to split water with use of a manganese cluster as catalyst, allowing hydrogen to travel along to the next steps in the process by way of cytochrome and photosystem I, responsible for energy storage in ATP and transfer of energy to outer side of the membrane for use in CO_2 assimilation [1]. The water splitting section of photosystem II (indicated by a rectangle in Figure 3) is shown enlarged in Figure 4. Like the PEM fuel cell, the organic system uses a membrane to keep products from recombining, and it also uses a catalyst as assistant to the basic water splitting.

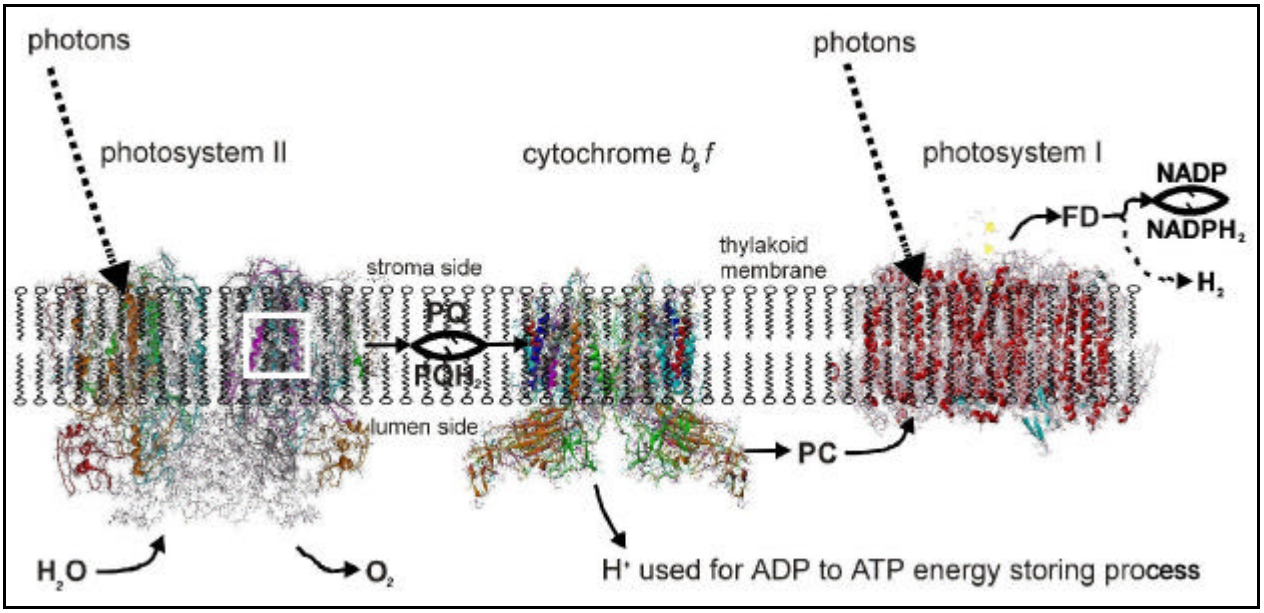

Figure 3. Schematic picture of the components of photosynthesis in plants and cyanobacteria [1,2,3,4]. The transfer by plastoquinone (PQ), plastocyanine (PC) and derredoxin (FD) is of interest for biological production of hydrogen, but here the emphasis is on the active area of photosystem II, indicated by a white rectangle enlarged in Figure 4.

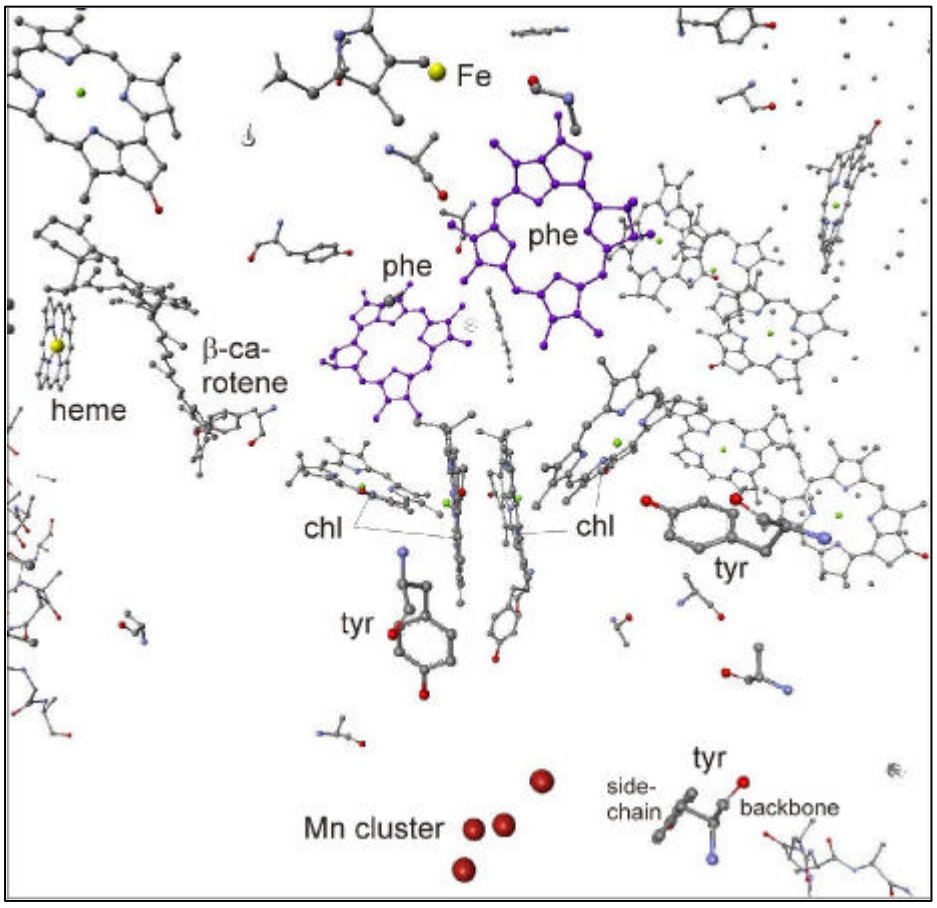

Figure 4. Central area of photosystem II, with amino acid chains omitted except for part of the tyrosine (*tyr*) molecules, that transfer energy from light harvesting chlorophylls (*chl*) to the area near the four Mn atoms, where water splitting takes place. Oxygen molecules are leaving towards the lower side of the picture view, while hydrogen ions are reducing a plastoquinone (PQ) cluster on the upper side (above the pheophytin *phe* in the picture) to PQH_2 [1,2].

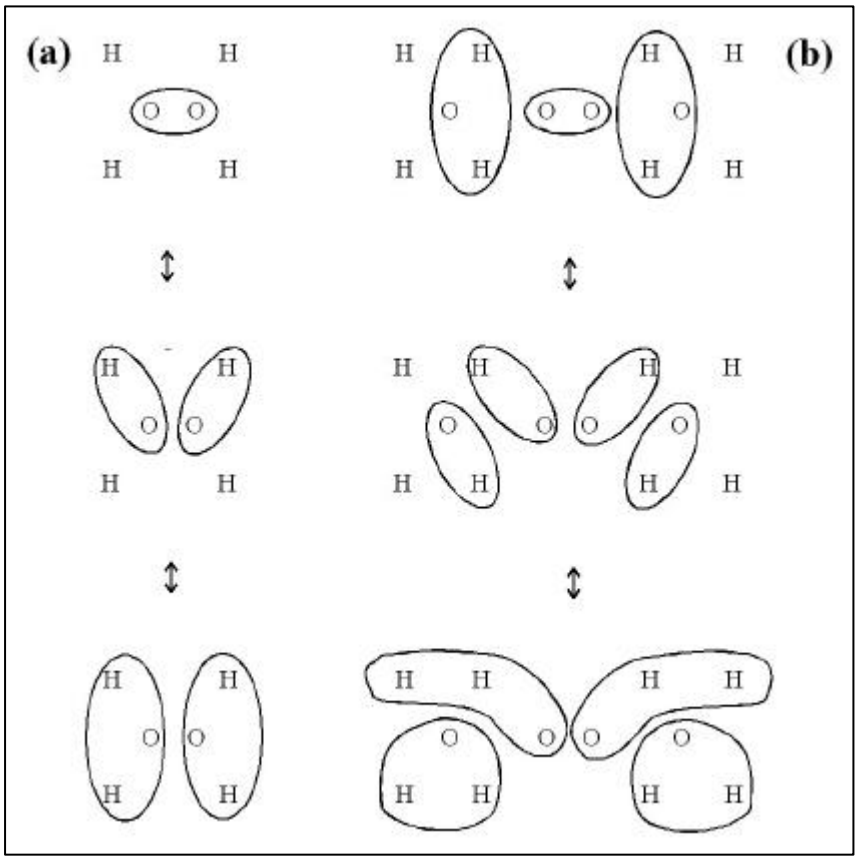

Figure 5. Proposed reaction mechanisms for water splitting in organic photosystem II (a) and in inorganic electrolysers and reverse fuel cell systems (b). See text for discussion.

The proposed mechanism for water splitting in photosystem II is one of sequential stripping of four protons one by one [6], illustrated in Figure 5(a). In electrochemical devices such as fuel cells, the process is considered to consist of two steps (Figure 5(b)):

$$4H_2O \rightarrow 4OH^- + 4H^+ \quad \text{and} \quad 4OH^- \rightarrow 2H_2O + O_2, \tag{1}$$

the overall reaction requiring an energy input of 288 kJ/mol in the liquid phase. In other words, the second proton is not able to directly leave the OH^- radical, but will form a new water molecule if another similar process can free another oxygen atom. The combination of the two oxygen atoms to an oxygen molecules (or the opposite process in normal fuel cell operation) requires the presence of a catalyst, such as Pt. The first step (bottom to middle line in Figure 5) is the same for organic and inorganic water splitting. The reason that the organic molecule in Figure 5(a) (middle to upper step) can get away with direct O_2 formation from just two OH^- radicals is, if this is the right explanation, that the molecules are held in place by the amino acid chains (capable of storing and releasing any supplementary energetic requirements), in conjunction with the action of the special cluster of four Mn atoms acting as the Pt (or Pt compound) catalyst does in the fuel cell. Early suggestions that Mn existed in photosystem II as oxides [7] have not been confirmed by the structural studies [2]. Although not all details are revealed at the resolution achieved (0.37 nm), it is unlikely that 8 oxygen atoms should have remained undetected near the 4 Mn atoms detected.

One purpose of the quantum mechanical calculations discussed below is to verify (or falsify) the above suggestions regarding reaction pathways.

2. The hydrogen terminal

The first realistic quantum chemical calculation showing the capability of metal catalysts such as Pt to split hydrogen molecules into protons and electrons was performed in 1995 [8]. Figure 6 shows the results of a similar calculation for hydrogen at a nickel surface. The [111] surface is modelled by two layers of a total of 24 atoms, which is enough to obtain the results at approximately the same accuracy as for larger models. There are 6 co-ordinates to vary for the two hydrogen atoms, but the main ones are the distance z from the Ni surface to the centre of mass of the two H atoms, and the separation a between the H atoms assumed to be at the same height over the surface, and at a constant angle relative to the lattice axes. The is some dependence on the position of the centre of mass relative to the Ni atom lattice (whether on top of atoms, on bridges between atoms or at the face centre between atoms), but the two-parameter surface shown in Figure 6 illustrates the preference to the H_2 molecule at larger distances (predicting the H-H distance correctly as 0.074 nm), as well as the splitting into two separate H atoms at a preferred distance from the Ni surface of 0.32 nm.

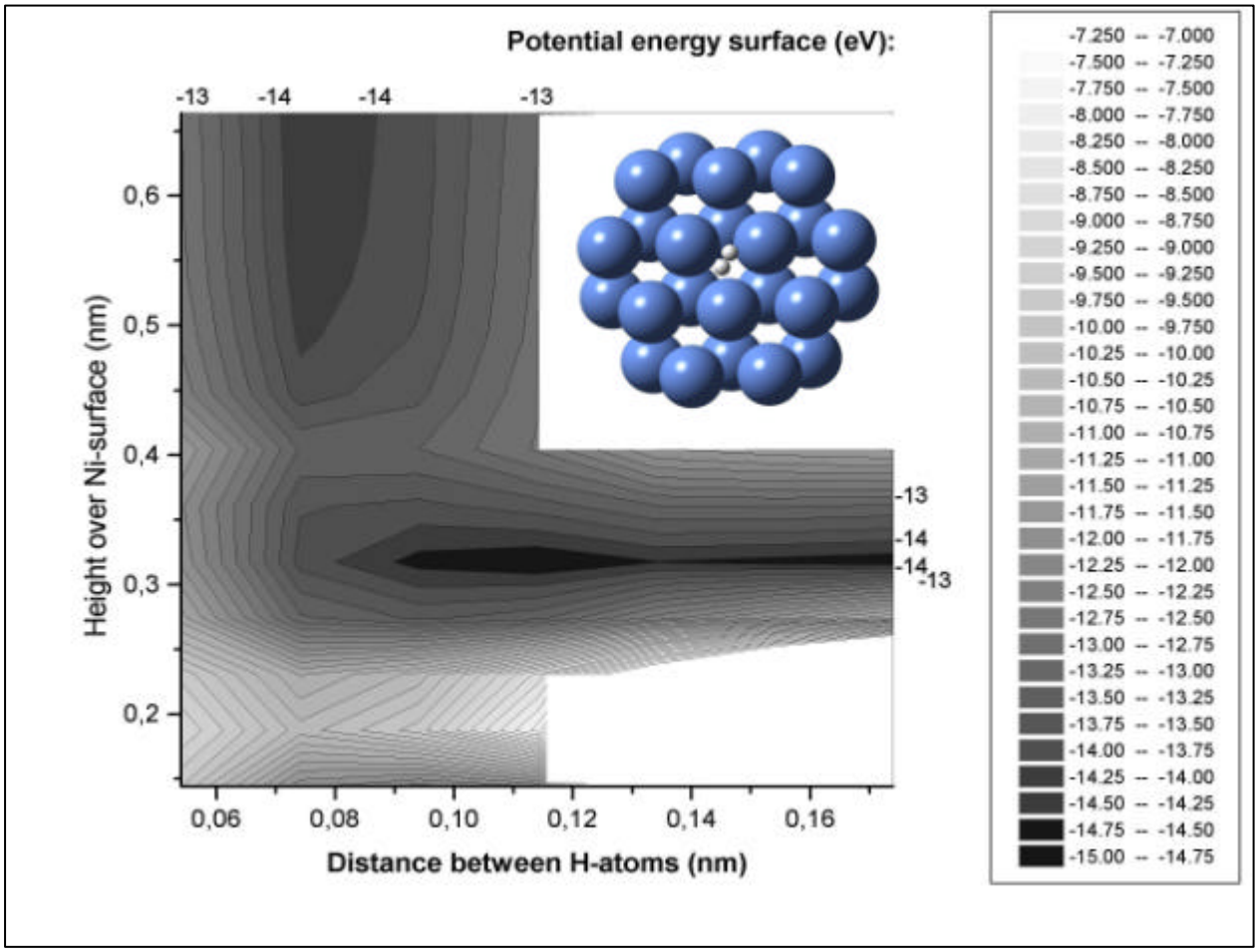

Figure 6. Potential energy surface of a two-layer Ni [111] lattice and two hydrogen atoms, as function of the H-atom-to-surface height and the separation between the H atoms [1].

Figure 6 gives the potential energy surface in eV. The kinetic energy of the hydrogen molecule or atoms will allow them to penetrate the finite quantum barrier between the two minima. The calculation uses a Gaussian function space based upon the orbital basis set SV [9], and calculates

ground state energies with use of the selfconsistent Hartree-Fock method, augmented by a density functional method (B3LYP) parametrising additional interaction such as the exchange force [10,11]. The reaction path takes the system across a barrier of approximately 10 eV, with the separated H state approximately 2 eV lower than the H_2 molecular state.

3. The oxygen terminal

Calculations of the ability of the Ni surface to catalyse splitting of an oxygen molecule into two oxygen atoms show a behaviour very similar to that of Figure 6, as demonstrated in Figure 7. The O_2 minimum for large distances over the surface occur at an O-O separation of 0.121 nm, in agreement with the experimental value of 0.1208. The two minima are not at the same depth (8.9 eV difference), and the barrier between them as seen from the O_2 side is only about 1.6 eV. The minimum occurring for a separation of the O atoms of about 0.145 nm, rather than a flat behaviour for larger separations, is due to the periodic structure of the underlying Ni surface, with preferred sites for chemisorption (the insert in Figure 7 shows the approximate O---O separation in the minimum). A similar behaviour is found for oxygen above Pd- and Pt-based surfaces [16].

A second calculation was made with two additional hydrogen atoms, placed on line with the oxygen atoms. In order to make the calculations comparable, the hydrogen atoms were also present in Figure 7, but at large distances of 0.9 nm from the oxygen centre of mass, making them insignificant for the relative potential surface. The effect of gradually moving the hydrogen atoms closer to the oxygen atoms is to make the O_2 minimum deeper (by as much as some 40 eV), but at the same time to make the separate atom O---O minimum disappear. Adding two further hydrogen atoms (at equal distance from one of the oxygen atoms and in the plane parallel to the Ni surface at a certain distance z) makes the O_2 minimum disappear, while the situation with the oxygen atoms separated stabilises with the hydrogen atoms attaching to each oxygen atom at the correct distance (0.096 nm). The distance to the Ni surface has to be around 0.40 nm in order for the oxygen atoms to split apart. These calculations confirm the existence of a number of relative minima (of different depths) corresponding to the expected configurations of the system. Additional calculations are needed with the 4 hydrogen atoms at unequal distances to the oxygen atoms, and of 4 oxygen atoms with 4 hydrogen atoms to represent the middle to upper transition in Figure 5(b).

Generally speaking, the mapping of the potential surface for the most complicated configurations considered in Figure 5 involves 4 oxygen atoms and 8 hydrogen atoms, i.e. 36 co-ordinates for independent variation. which at the moment is computationally out of reach, even with a crude scan of some 5-10 values for each variable. This is why the calculation is restricted to constrained configurations judged of interest, and done in batches, refining the surface in regions found interesting and neglecting complications not deemed important. There is the alternative method of following the reaction path in steps from the transitional saddle point state (finding e.g. the direction of steepest descent), but this requires identification of the transition point, which means first doing the potential scan as outlined. With this done, the reaction-following calculation (in both directions from the saddle point) does not add much new, and may be expensive due to the smallness of steps taken when the routine used detects ambiguity due to numerical uncertainty.

The calculations discussed so far have not included the distribution of charges over the entire system of Ni, O and H atoms, although each calculation of course predicts an electron density distribution. For electrolysis, energy has to be added by applying a voltage across the external circuit between the electrodes. This means having a surplus of electrons migrate to the Ni surface of the hydrogen producing side of the membrane, and away from the Ni surface on the oxygen side. This situation can be modelled explicitly, by dividing the system into the Ni cluster and one

or two systems for the components of the water molecules. For example, the H atoms in Figure 5 not encircled may be given a positive charge (zero electrons). The situation at the top of the Figure requires only positive charges on hydrogens, and the situation at the bottom then requires only a positive charge (of 4) on the Ni cluster. This means that in the biological case, the intermediate situation is one where there are still 2 charges on the Ni cluster, while in the fuel cell case, the OH entities have no overall charge, which is a modification of the classical reaction (eq. 1) needed to explain the electron motion in the external circuit (and a reasonable one, as the OH's do not need to move and thus not to be ions, and as the role of the metal surface is much more explicit with the electrons requiring the metal surface to transfer to).
Technically, the division of the system into differently charged subsystems in the quantum chemical calculations are made by using the ONIOM method [12] (originally devised for using semi-classical methods for some part of the system). This method calculates the quantum state of each subsystem with a summary consideration of the other subsystems, allowing an approximate estimate for the total energy to be made at the end. In the case considered here, this method precisely allows each subsystem to be modelled with a prescribed total charge, implying that the ionic traits of the different configurations discussed above can be followed.

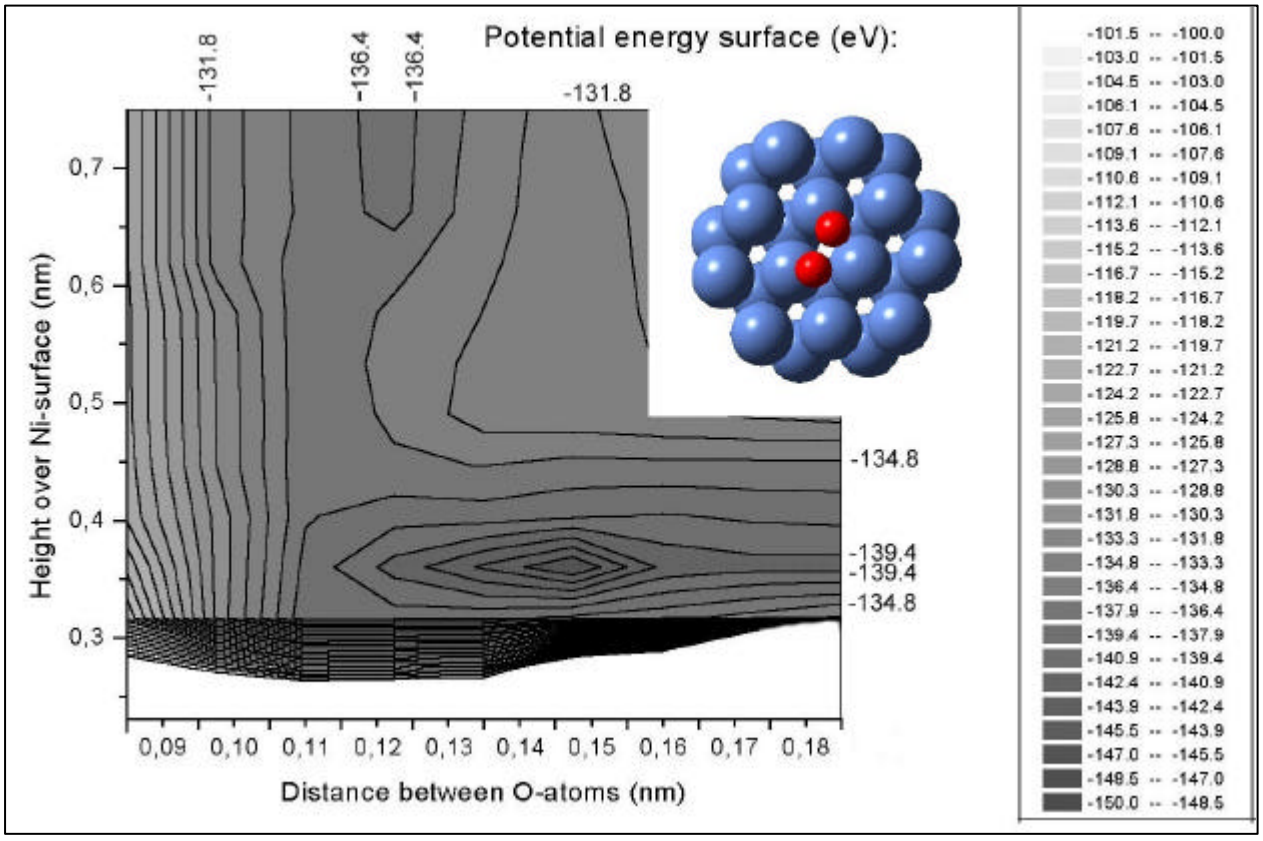

Figure 7. Potential energy surface of a two-layer Ni [111] lattice and two oxygen atoms, as function of the height of the O atoms over the Ni surface and the separation between the O atoms [1].

4. Concluding remarks

The Nafion [5] membrane illustrated in Figure 2 can be subjected to quantum chemical optimisation, in order to find the likely shape of a molecule or conglomerate of molecules (for computational reasons hardly bigger than 4-8 units, at the currently available level of computer power).

There is experimental evidence [13,14] that Nafion forms layers of fairly uniformly arranged nodules, and models have been suggested, with a cross section (cf. Figure 2) where the upper and lower backbone membranes each form a semi-circle to enclose a number of sidechains and water molecules. In three dimensions, these features become half-spheres, and the interesting thing in the proposed structure is that between the spheres, two layers of membrane backbones simply form a double layer with no sidechains [15]. The number of CF_2 segments between sidechains may vary from 6 to about 12. Ongoing calculations aim to demonstrate the process of curling up.
The next question is whether the polymer membrane has any influence on the water splitting process, other than to carry H^+'s away to the other electrode. Recent experiments on direct methanol fuel cells suggest, that the Nafion membrane indeed co-operates with the electrochemical process [17]. It is also known, that the system only functions with the membrane soaked in water, and it is therefore of interest to explore what role the additional water molecules have in a quantum chemical simulation of a system such as the one shown in Figure 2.
The work outlined as ongoing or planned will be reported in [1] and other future publications.

5. References

[1] Sørensen, B. (2005). Hydrogen and Fuel Cells. Academic Press/Elsevier Science (under preparation).

[2] Protein Data Bank 1IZL; Kamiya, N. and Shen, J-R. (2003). Crystal structure of oxigen-evolving photosystem II from *Thermosynechococcus vulcanus* at 3.7-Å resolution. *Proc. Nat. Acad. Sci.* (US), **100**, 98-103.

[3] Protein Data Bank 1UM3; Kurisu, G., Zhang, H., Smith, J., Cramer, W. (2003). Structure of the cytochrome b6f complex of oxygenic photosynthesis: tuning the cavity. *Science*, **302**, 1009-1014.

[4] Protein Data Bank 1JBO; Jordan, P., Fromme, P., Witt, H., Klukas, O., Saenger, W., Krauss, N. (2001). Three-dimensional structure of cyanobacterial photosystem I at 2.5 Å resolution, *Nature*, **411**, 909-917.

[5] Nafion is a registered trademark of E. I. du Pont de Nemours & Co., North Carolina, USA.

[6] Barber, J. (2002). Photosystem II: a multisubunit membrane protein that oxidises water. *Current Opinion in Structural Biology*, **12**, 523-530; Kok, B., Forbush, B., McGloin, M. (1970). *Photochem. Photobiol.*, **11**, 457.

[7] Hoganson, C., Babcock, G. (1997). A metalloradical mechanism for the generation of oxygen from water in photosynthesis. *Science*, **277**, 1953-1956.

[8] Hammer, B., Nørskov, J. (1995). Electronic factors determining the reactivity of metal surfaces. *Surface Sci.*, **343**, 211-220.

[9] Schaefer, A., Horn, H., Ahlrichs, R. (1992). *J. Chem. Phys.*, **97**, 2571.

[10] Becke, A. (1993). *J. Chem. Phys.*, **98**, 5648.

[11] Software used: Weblab Viewerlite 3.7, Origen 5, Gaussian 03 (the complete list of contributors to the last package is given at http://www.gaussian.com).

[12] Dapprich, S., Komáromi, I., Byun, K., Morokuma, K., Frisch, M. (1999). A new ONIOM implementation in Gaussian98. Part I. The calculation of energies, gradients, vibrational frequencies and electric field derivatives. *J. Mol. Struct.*, **461-2**, 1-21.

[13] Elliott, J., Hanna, S., Elliott, A., Cooley, G. (2000). Interpretation of small-angle X-ray scattering from swollen and oriented perfluorinated ionomer membranes. *Macromolecules*, **33**, 4161-4171.

[14] Barbi, V., Funari, S., Gehrke, R., Scharnagl, N., Stribeck, N. (2003). Nanostructure of Nafion membrane material as a function of mechanical load studied by SAXS. *Polymer*, **44**, 4853-4861.

[15] Vankelecom, I. (2002). Polymeric membranes in catalytic reactors. *Chem. Rev.*, **102**, 3779-3810

[16] Yamaguchi, Y., Tabata, K., Suzuki, E. (2003). Density functional theory calculations for the interaction of oxygen with reduced $M/SnO_2(110)$(M=Pd,Pt) surfaces. *Surface Science*, **526**, 149-158.

[17] Chu, Y., Shul, Y, Choi, W., Woo, S., Han, H. (2003). Evaluation of the Nafion effect on the activity of Pt-Ru electrocatalysts for the electro-oxidation of methanol. *J. Power Sources*, *118*, 334-341.